Sound & Vibration 2025, 59(1), 1998.
https://doi.org/10.59400/sv1998

Article

Analysis of characteristics of ground motion and typical bridge performance in the Baoshan earthquake

Yong Huang[1,2,*], Liang Tian[1,2], Yachen Xie[1,2], Yuexiang Wu[1,2]

[1] Key Laboratory of Earthquake Engineering and Engineering Vibration, Institute of Engineering Mechanics, China Earthquake Administration, Harbin 150080, China
[2] Key Laboratory of Earthquake Disaster Mitigation, Ministry of Emergency Management, Harbin 150080, China
*** Corresponding author:** Yong Huang, huangyong@iem.ac.cn

CITATION

Huang Y, Tian L, Xie Y, Wu Y. Analysis of characteristics of ground motion and typical bridge performance in the Baoshan earthquake. Sound & Vibration. 2025; 59(1): 1998. https://doi.org/10.59400/sv1998

ARTICLE INFO

Received: 7 November 2024
Accepted: 20 November 2024
Available online: 10 December 2024

Abstract: A Ms5.2 earthquake occurred in Longyang District, Baoshan City, Yunnan Province on 2 May 2023. The earthquake caused some degree of damage to power facilities and roads. Since then, small and medium sized earthquakes have occurred frequently in this region. In order to better analyze the characteristics of ground motion in this area and the coping strategies of related bridges, the response spectra, omnidirectional response spectra and omnidirectional representations of other indexes of intensity measure from records of strong ground motion were analyzed using the seismic records recorded by stations near the epicenter. Four typical bridges near the epicenter were selected for modeling and seismic response analysis to derive their damages under the action of ground motion, and structural displacements of the bridges with the strong ground motion were compared to analyze directional linkages. The Incremental Dynamic Analysis (IDA) method was used to analyze the fragility of the four bridges, and the seismic capacity of different bridges under the ground motion was compared. The omnidirectional displacement response spectra of the two stations and the omnidirectional representations of other indexes of intensity measure have obvious directionality, and the predominant direction is perpendicular to the direction of the fault, reflecting the rupture directionality of the earthquake. Comparing the corresponding period of the structural displacement response with seismic action with the omnidirectional displacement response spectra, it was found that the bridge structural displacement is correlated with the predominant cycle and predominant direction of the omnidirectional displacement response spectra. Under the same seismic action, the maximum moment of the deck arch bridge in the transverse direction is larger than that in the bridge direction; the larger the span of the deck arch bridge, the larger the maximum moment at the arch footing. According to the analysis of fragility, it can be seen that the seismic capacity of the continuous rigid frame bridge is much lower than that of the deck steel truss arch bridge under this ground motion. Compared to the deck-type concrete arch bridge, the deck steel truss arch bridge has greater seismic capacity. In this paper, based on the structural analysis and fragility analysis of these four bridges close to the fault, the structural damage and damage levels in the future earthquake are speculated, which provide suggestions for the follow-up maintenance and reinforcement work, and are also conducive to the resilience evaluation and rapid repair work after the real earthquake damage.

Keywords: Baoshan earthquake; strong ground motion records; transport system; near-fault ground motion; fragility

1. Introduction

1.1. Seismic damages

According to the China Earthquake Networks Center [1], at 23:27 on 2 May 2023, a Ms5.2 earthquake occurred in Longyang District, Baoshan City, Yunnan Province (latitude 25.35 degrees north, longitude 99.28 degrees east), the focal depth is 10 km. The earthquake's maximum intensity zone covers an area of approximately 600 km^2. The seismic faults are strike-slip faults.

The epicenter is about 29 km away from Longyang District, about 28 km away from Yongping County, about 61 km away from Yunlong County, about 66 km away from Changning County, about 70 km away from Shidian County, and about 347 km away from Kunming. The China Earthquake Early Warning Network (CEWN) issued early warning information 9 s after the earthquake, and 656 early warning terminals and 219,000 TV users received early warning information. The earthquake was strongly felt in Baoshan and Dali, Lincang, Nujiang and other places also have a sense of earthquake. There were rolling stones, cracked walls and shuttle tiles and so on at the epicenter. As of 1:23 p.m. on 3 May, there were 38 aftershocks.

After a preliminary investigation, as of 5 p.m. on 3 May, the earthquake had caused minor injuries to three people, who had been sent to hospital for treatment, without life-threatening injuries. The earthquake caused various degrees of damage to the epicenter of the earthquake and the surrounding residential buildings and infrastructure related to water, electricity, roads, communications, and so on. After a preliminary investigation, the specific damages are as follows:

Damages to electrical facilities: Due to the earthquake caused 110 kV Wayao substation and Lao Ying substation each 10 kV line failure outage, the power load was lost by 700 kW. Five small hydroelectric power stations in Wayao area, namely, Wayao three-stage power station, Wayao four-stage power station, Wanpa River power station, Zhonghe power station and Xueshan River power station, stopped generating electricity.

Damages to the roads: Rockfall is found at K2694 + 330 of K2689-K2691 section of Dabao Expressway, the K2690 + 160 (Eagle Rock) bridge in the K2689-K2691 section of Dabao Expressway was damaged by rockfall. The Yongbao Bridge K3280 + 100 to Laoying K3320 + 100 (40 km) section of the provincial highway G320 line has a small amount of rockfall, which affects the traffic. The road waveform guardrail of County Road Wafang to Wayao has 100 m of damage, falling rocks damaged road surface 1000 m^2. The bridge deck and arch of Hetaoping River Bridge in county road are damaged. The multi-section damage of the township maintenance road in Wayao Town affects the traffic. The Hangzhou-Ruili Expressway, which was interrupted by the earthquake has been restored to traffic. The temporary traffic control of Laoying-Cangjiang section of Hangzhou-Ruili Expressway was lifted at 03:40 on 3 May, and the road from Dali to Baoshan returned to normal traffic. Small vehicles in the direction from Baoshan to Dali resumed traffic. Due to the damage of the pavement of K2690 Eagle Rock No.1 Bridge, the large trucks do not have the conditions for passage. The large trucks in the direction of Baoshan to Dali need to detour through the expressway.

1.2. Directionality-related research

According to the rapid report catalog of China Earthquake Networks Center, 123

earthquakes with magnitude greater than 3 have occurred within 200 km around the epicenter in the past 5 years. The earthquake with maximum magnitude was an earthquake of magnitude 6.4 that occurred in Yangbi County, Dali Prefecture, Yunnan Province on 21 May 2021, which is 69 km from the current epicenter. another earthquake of magnitude 3.2 occurred on 28 December 2023 in Shidian County, Baoshan City.

In recent years, small and medium sized earthquakes have occurred frequently in this region. From 2 May 2023 onwards, a number of earthquakes occurred in the region. An earthquake of magnitude 2.9 occurred on 18 September 2023, an earthquake of magnitude 3.2 occurred on 28 December 2023, an earthquake of magnitude 3.6 occurred on 29 July 2024; and an earthquake of magnitude 3.4 occurred on 25 August 2024. It is of great significance to explore the directionality of ground motion and characteristics of performance of typical bridges in this region with the earthquake of magnitude 5.2 in 2023 as an analytical case to formulate corresponding seismic countermeasures and to improve the seismic fragility of bridge structures.

The directional characteristics of regional ground motion and the characteristics of response of bridges have been studied as follows:

Wang et al. [2] studied the seismic performance of bridges with pier heights of 100 m under near-fault ground motion. The relationship between the longitudinal direction of the bridge and the direction of the fault affects the seismic response of the bridge in relation to the specific input ground motion, and the bridge can be damaged even if the design meets the specifications.

Bao [3] studied the response of simply supported girder bridges under the action of near-fault ground motion and concluded that when the peak value of ground motion is the same, the forward direction effect and fling-step effect cause an increase in displacement of the top of piers, shear and bending moment of the bottom of piers and shear of the bearings.

Hu et al. [4] analyzed 198 sets of three-component ground motions recorded on similar soil site conditions from Wenchuan earthquake, quantitatively compared and analyzed the peak values, response spectra, and duration of ground motion perpendicular to faults, parallel to faults and vertical components in the pre-rupture and post-rupture directions. The directionality of the rupture propagation was found such that the peak values, response spectra and duration of the ground motion all exhibited significant directional characteristics.

Li et al. [5] took the near-fault ground motions of the Taiwan Chi-Chi earthquake as the object of study. A cable-stayed bridge with a main span of 406 m was used as the relying project, and a comparative study on the law of seismic response with the effect of ground motion in the Forward District, the Middle District and the Backward District was carried out.

Zhang et al. [6] investigated the response of a large-span cable-stayed bridge under near-fault ground motion with different characteristics, and concluded that the fling-step effect significantly increases the magnitude of the change in bending moment and longitudinal displacement of the main tower, and shear of the main tower.

Xie et al. [7] investigated the directional properties of near-fault ground motion during the 7.0 earthquake of magnitude 7.0 in Lushan based on the strong ground motion records from stations with a distance of less than 100 km from the fault, and

found that the ground motion has an obvious directionality within a distance of about 35 km from the fault, and the predominant direction of ground motion has the characteristic of being perpendicular to the fault, which is not obvious with the increase of the distance from the fault.

An et al. [8] studied the spatial distribution and attenuation characteristics of near-field strong ground motion of the Hualien MW6.4 earthquake, investigated the differences in peak ground acceleration, peak velocity, and the spatial distribution of ground motion with different periods based on regression residual analysis, and quantitatively analyzed the directional effects of ground motion, and found that the directional effects of rupture propagation mainly affect the long period which is more than 1.0 s, while the effect on PGA and short-period ground motion with periods less than 1.0 s is weak.

Sun et al. [9] found that the directionality of the ground motion input has a greater effect on the response of structures with asymmetric mass-stiffness.

Zhao et al. [10] quantitatively investigated the directional properties of near-fault ground motion of the 2018 Hualien earthquake in Taiwan, and its relationship with the rupture mechanism of the seismic source, the distance from the fault and the spatial orientation. The difference in the directionality of ground motion increases with increasing period, and the ground motion has obvious directionality within 30 km of distance from the fault, and the preeminent direction of ground motion is closest to the direction perpendicular to the fault near the Milun Fault within 5 km of the distance from the fault; the preeminent direction of ground motion is highly coincident with the direction of the relative movement of the fault in the segments of longer period.

Li [11] studied the directional characteristics of near-fault ground motion under different site conditions by classifying earthquakes according to their sites and using omnidirectional response spectra.

In order to study the characteristics of this earthquake and to know the response of different types of bridges in the earthquake, the characteristics of the ground motion were analyzed by studying the strong ground motion records measured by 6 stations near the epicenter and the response spectra obtained from the strong ground motion records. The finite element modeling of four typical bridges near the epicenter was carried out, and the seismic response analysis was carried out. Analysis of fragility were done for these four bridges to study their structural responses which are more likely to be affected by ground motion.

2. Characteristics of strong ground motions of earthquake

2.1. Location of the stations

Six stations with effective seismic information measured near the epicenter are YPX station, BSL station, LKT station, SDX station, DLY station and LLP station. The location of each station and the epicenter is shown in **Figure 1**, and the distance between each station and the epicenter is shown in **Table 1** (The epicenter is marked in black, bridges in blue, stations in red, intensity in blue lines and faults in red lines).

Figure 1. Location of stations and epicenter.

Table 1. Distance between each station and epicenter (km).

Station	YPX	BSL	LKT	SDX	DLY	LLP
Distance between each station and epicenter	27.8	28.9	62.8	72.7	100.2	211.1

The largest PGA was recorded at the BSL station, and the three components of EW, NS, and UD are 28.296 cm/s^2, 40.205 cm/s^2, and 35.408 cm/s^2, respectively.

The PGA recorded by YPX station is also larger, and its EW, NS and UD components are 35.0006 cm/s^2, 32.601 cm/s^2 and 27.997 cm/s^2, respectively.

According to the seismic records and the fault distribution analyzed by the Yunnan Earthquake Agency, it can be seen that the BSL station and the YPX station, which recorded the larger PGA, are located in the near-fault region.

2.2. Analysis of the characteristics of strong ground motion recorded by stations

In order to better grasp the characteristics of ground motion, this paper adopts the method proposed by Inoue et al. [12] for the analysis of omnidirectional response spectra. Acceleration time history, response spectra, and omnidirectional response spectra corresponding to the strong motion recorded by each station are derived [13].

It was observed that the most pronounced directionality was in the omnidirectional response spectra derived from the YPX and BSL stations closest to the epicenter, as shown below.

As shown in **Figure 2**, the acceleration time history of YPX station has the largest PGA in the east-west direction, followed by the north-south direction, and the PGA is similar. The predominant direction of omnidirectional acceleration response spectrum and omnidirectional velocity response spectrum are all northwest-southeast. The predominant cycle of the omnidirectional acceleration response spectrum is 0.25 s, and the predominant cycle of the omnidirectional velocity response spectrum is 0.8 s. Combined with the relative positions of the YPX station and the epicenter in **Figure 2**, the fling-step effect of the ground motion is reflected. The omnidirectional acceleration response spectrum is predominantly orientated vertically at the northern end of the fault at 0.1 s, and to some extent parallel to the central part of the fault at

0.25 s. The omnidirectional velocity response spectrum is predominant in the north direction near 0.75 s, and in the fault-parallel direction at 0.75 s–0.1 s. The omnidirectional displacement response spectrum has a tendency to change from parallel to vertical faults in the 0.5 s–1.0 s excellence direction.

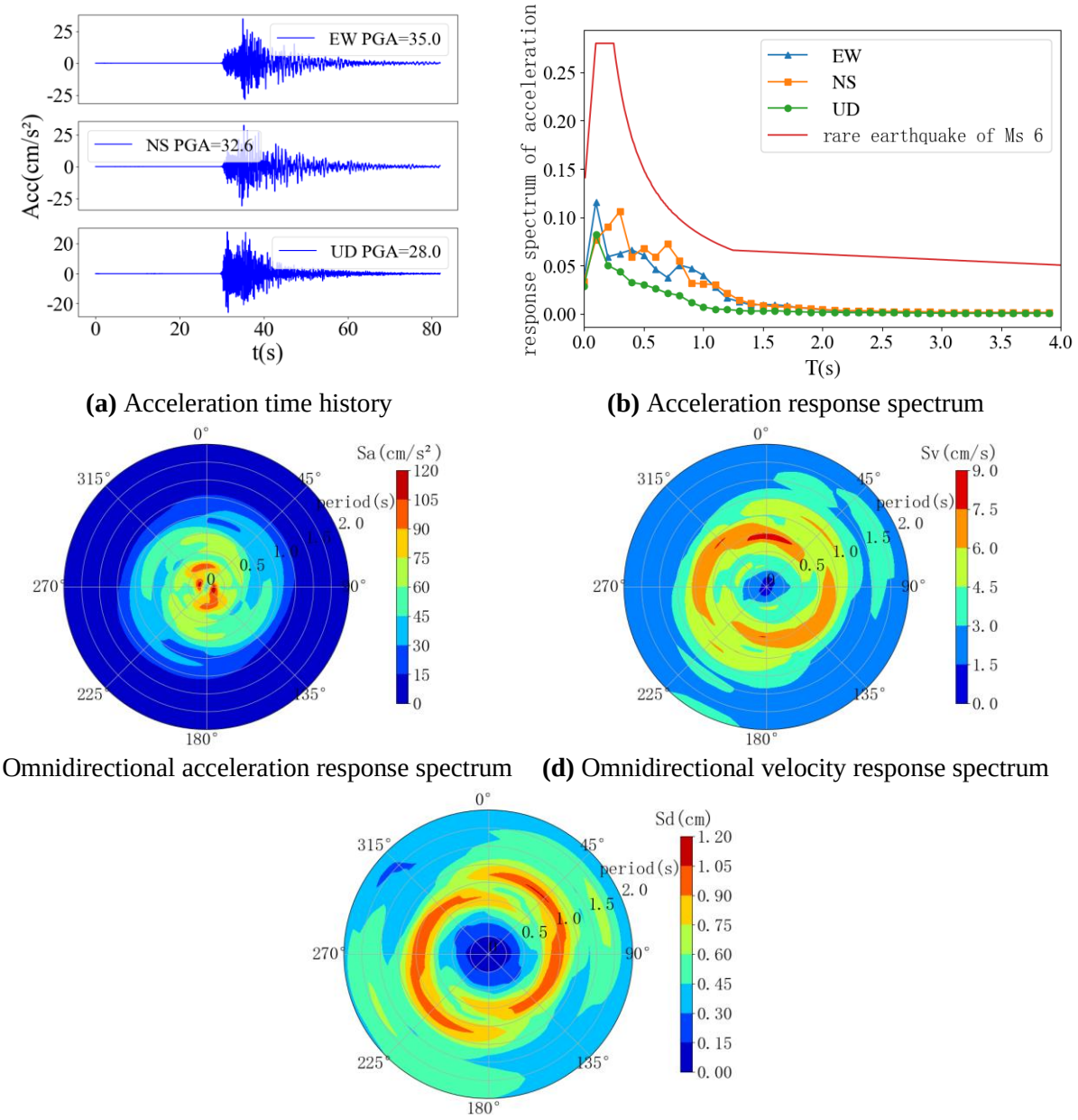

(a) Acceleration time history

(b) Acceleration response spectrum

(c) Omnidirectional acceleration response spectrum

(d) Omnidirectional velocity response spectrum

(e) Omnidirectional displacement spectrum

Figure 2. Acceleration time history, response spectrum and omnidirectional response spectrum corresponding to strong motion records of YPX station.

In addition, there are omnidirectional representations of other indexes of intensity measure from ground motion records, as shown in the **Figure 3**, where the red straight line indicates the direction of the fault [14,15].

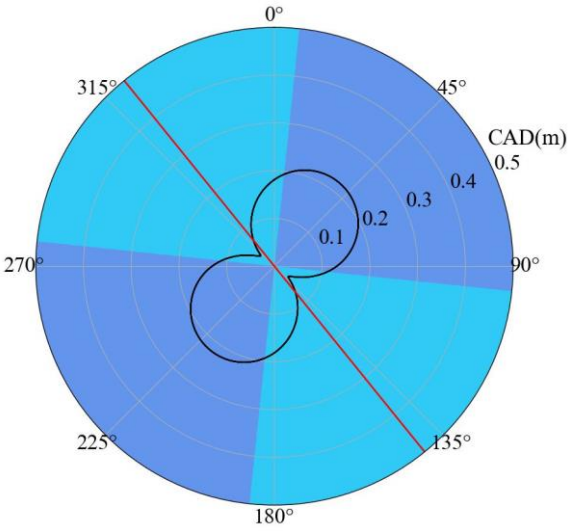

(a) CAD

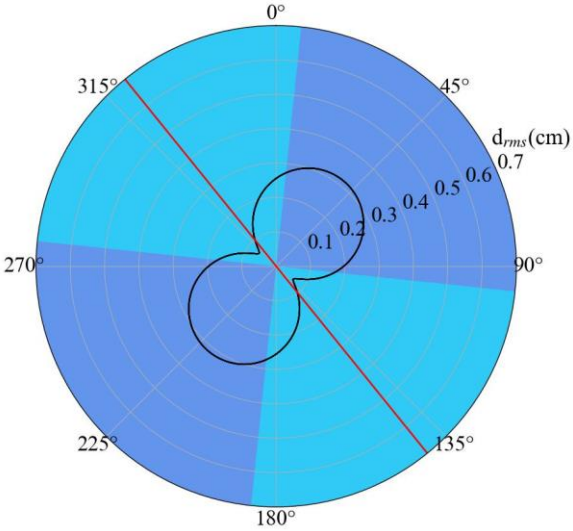

(b) Drms

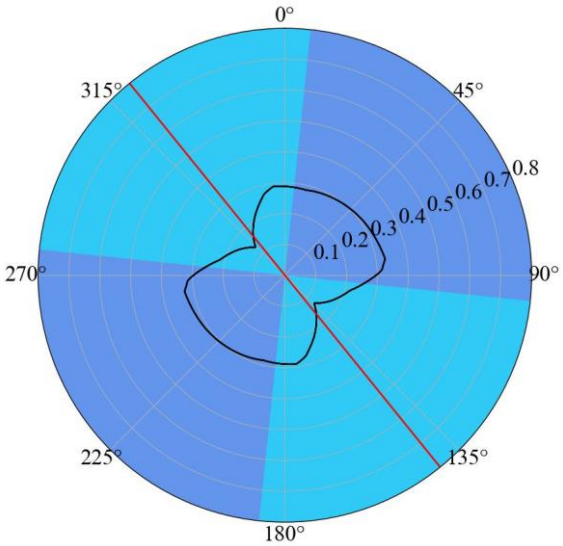

(c) D/V

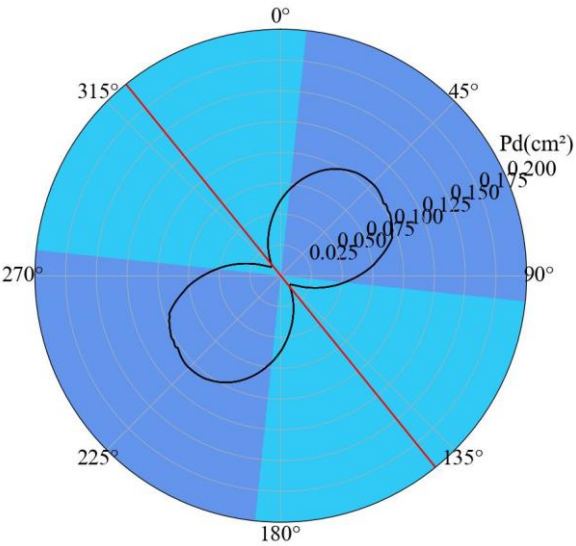

(d) HPD

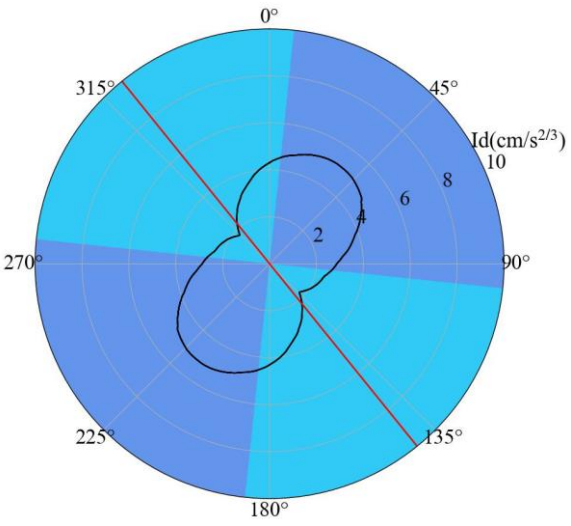

(e) Id

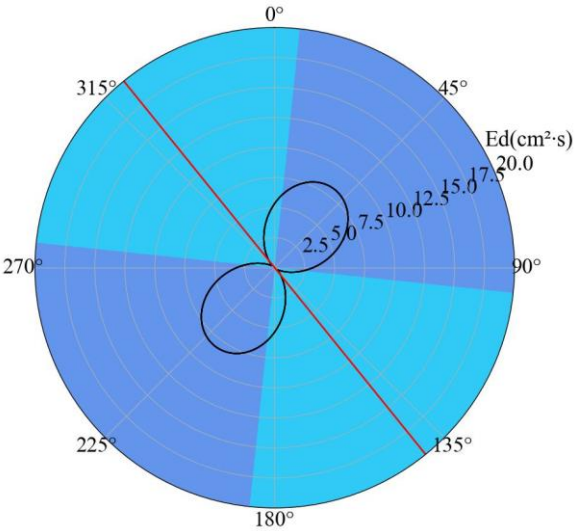

(f) NED

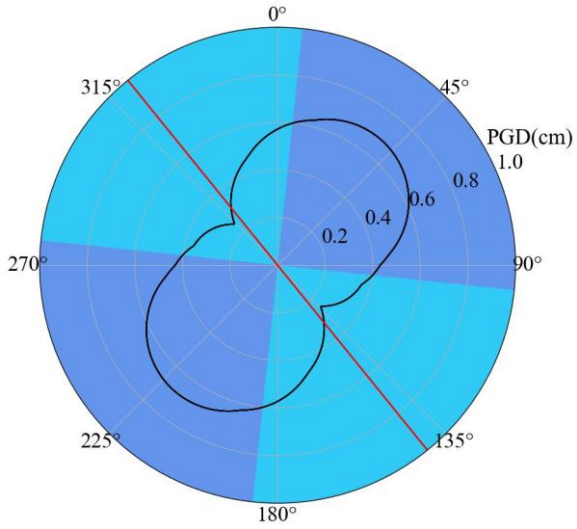

(g) PGD

Figure 3. Omnidirectional representation of some displacement-related indexes with obvious and identical directionality from YPX station.

Among them, the omnidirectional representation of displacement-related indexes such as CAD (cumulative absolute displacement), Drms (root-mean-square displacement), D/V (PGD/PGV), HPD (Housner's intensity), Id (composite indicator of displacement), NED (Nau and Hall's indicator Ed), PGD (peak ground displacement), etc., has an obvious and the same directional manifestation, i.e., it is nearly vertical to the fault direction, which reflects the rupture directionality of ground motion.

As shown in the **Figure 4**, the acceleration time history of BSL station has the largest PGA in the north-south direction, followed by the vertical direction. The predominant direction of omnidirectional acceleration response spectrum and omnidirectional velocity response spectrum are both northeast-southwest, the predominant cycle of the omnidirectional acceleration response spectrum is 0.25 s, and the predominant cycle of omnidirectional velocity response spectrum is 0.4 s. The predominant direction at 0.38 s of omnidirectional velocity response spectrum and the predominant direction at 1.8 s of the omnidirectional displacement response spectrum at are close to the vertical direction of the fault. The omnidirectional acceleration response spectrum has a similar trend, but the high-frequency predominant direction is more northerly.

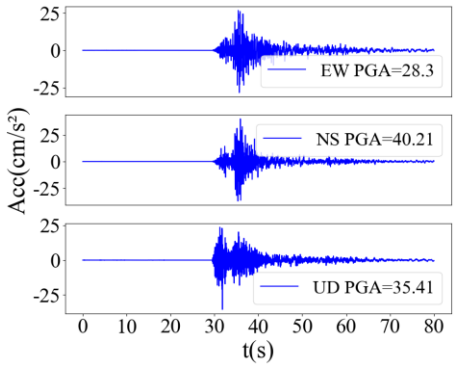

(a) Acceleration time history

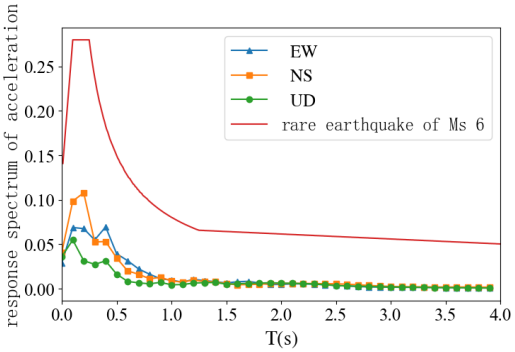

(b) Acceleration response spectrum

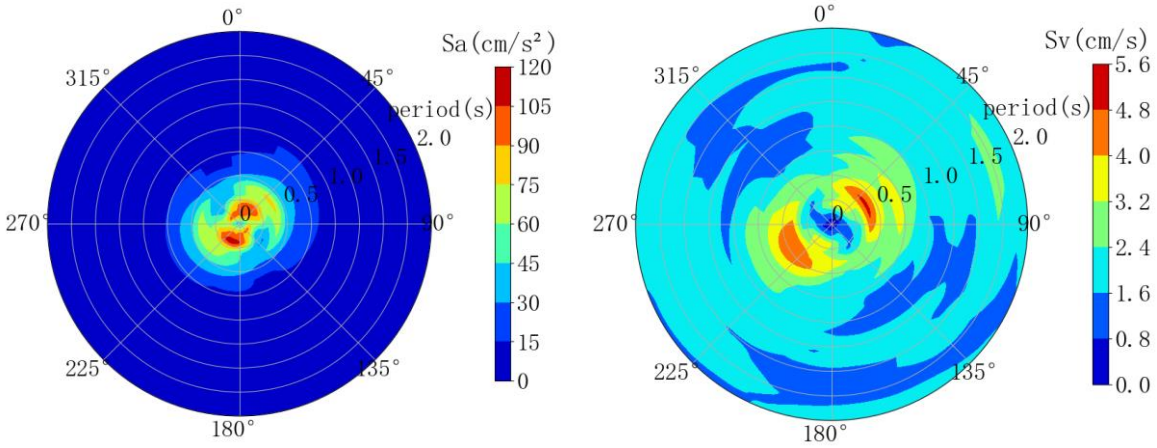

(c) Omnidirectional acceleration response spectrum **(d)** Omnidirectional velocity response spectrum

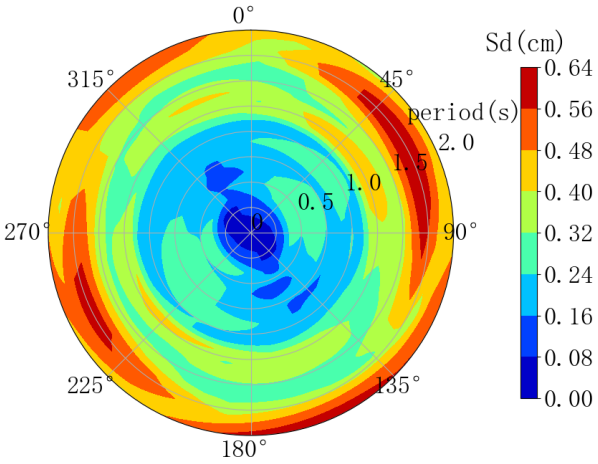

(e) Omnidirectional displacement spectrum

Figure 4. Acceleration time history, response spectrum and omnidirectional response spectrum corresponding to strong motion records of BSL station.

There are omnidirectional representations of other indexes of intensity measure from ground motion records, as shown in the **Figures 5** and **6**, where the red straight line indicates the direction of the fault.

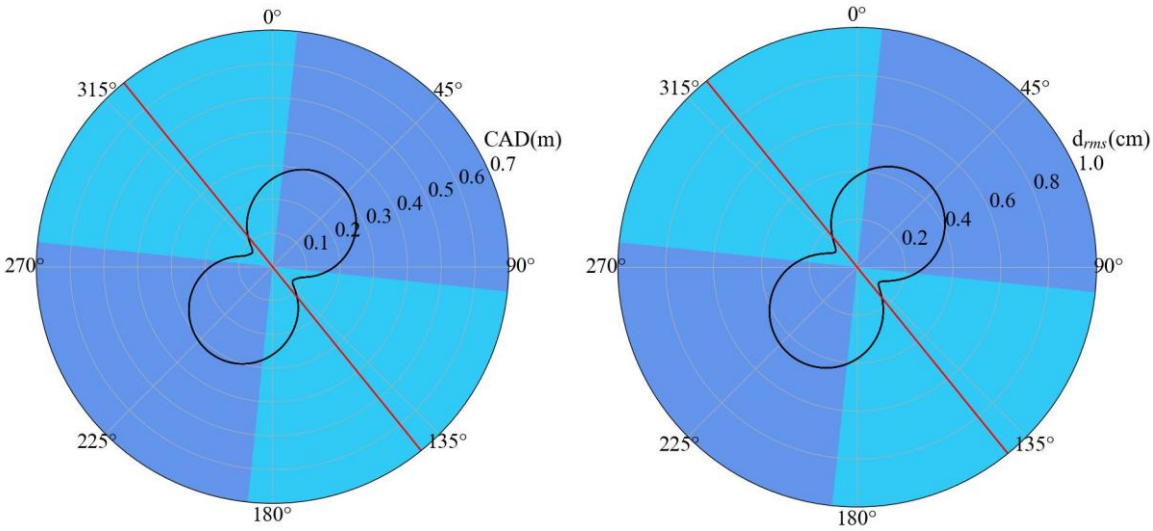

(a) CAD **(b)** Drms

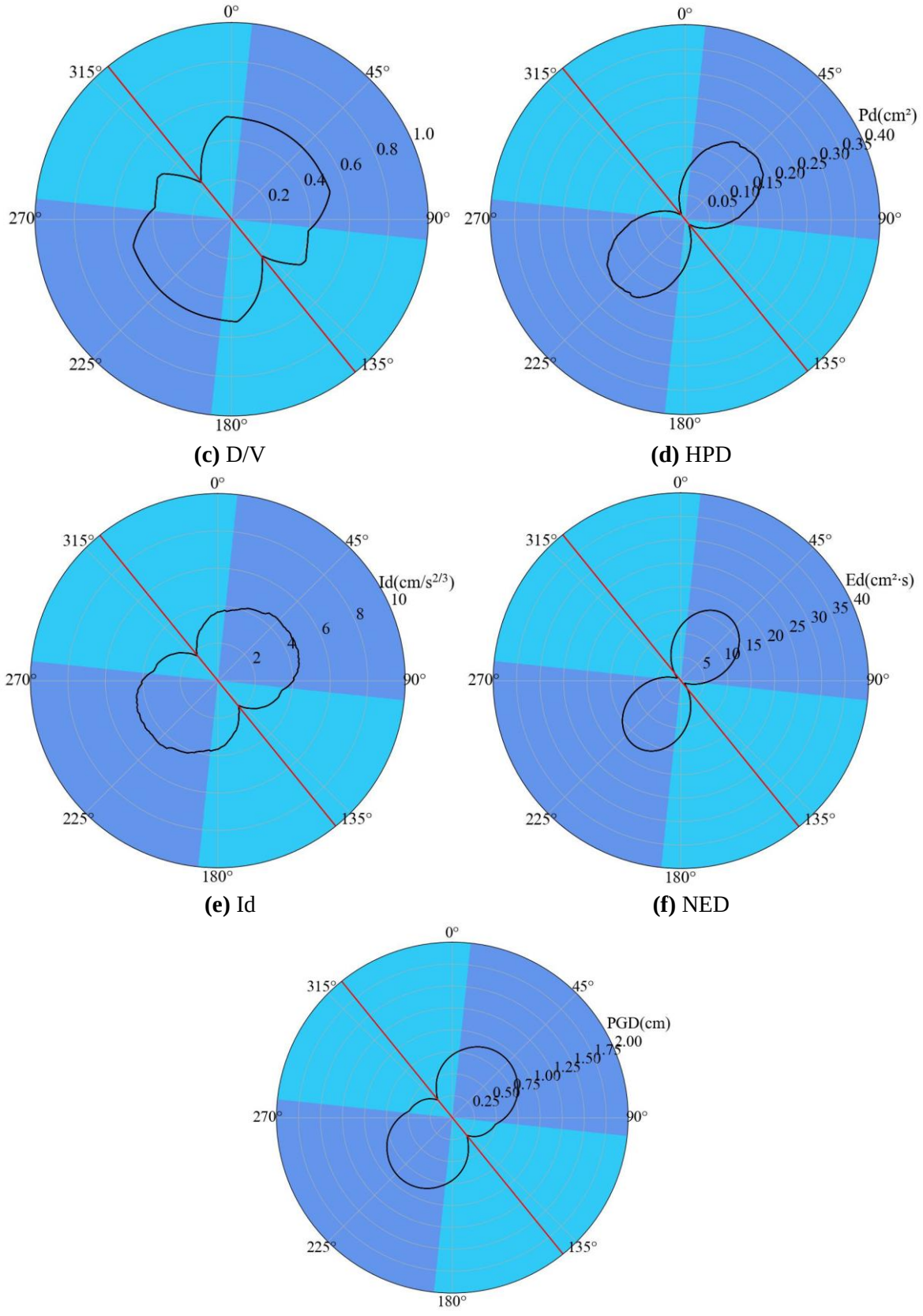

(c) D/V **(d)** HPD

(e) Id **(f)** NED

(g) PGD

Figure 5. Omnidirectional representation of some displacement-related indexes with obvious and identical directionality from BSL station.

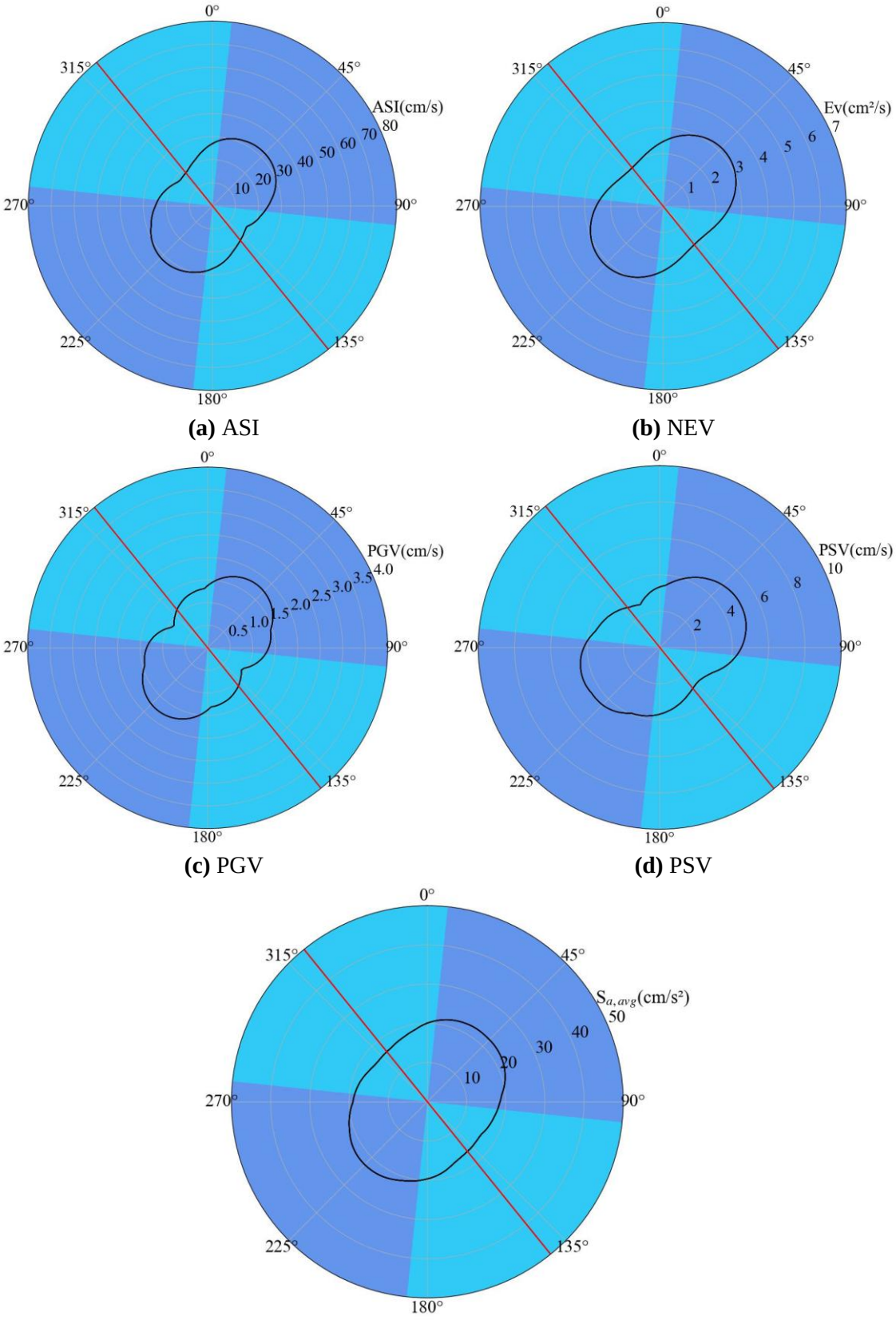

(a) ASI **(b)** NEV

(c) PGV **(d)** PSV

(e) Saa

Figure 6. Omnidirectional representations of non-displacement-related indexes with obvious and identical directionality from BSL station.

Among them, the omnidirectional representation of displacement-related indexes such as CAD (cumulative absolute displacement), Drms (root-mean-square displacement), D/V (PGD/PGV), HPD (Housner's intensity), Id (composite indicator of displacement), NED (Nau and Hall's indicator Ed), PGD (peak ground displacement) and the omnidirectional representations of indexes such as ASI (acceleration response spectral intensity), NEV (Nau Hall indicator Ev), PGV (peak ground velocity), PSV (peak spectral velocity), Saa (geometric mean spectral acceleration), etc. have obvious and identical directionality, i.e., approximately perpendicular to the direction of fault, which reflects the rupture directionality of the ground motion.

The omnidirectional acceleration response spectrum of BSL station has obvious directivity, and the predominant direction is northeast-southwest. The omni-directional representation of displacement-related ground motion indicators, such as cumulative absolute displacements, has a clear and identical directional behavior, which is approximately perpendicular to the direction of the fault, which is a clear indication of the rupture directionality of the ground motion.

3. Seismic response analyses for four typical bridges near the epicenter

The bridge damage in this earthquake was mainly caused by falling rocks hitting the Laoyingyan No.1 Bridge, which led to the destruction of the bridge deck, while the strong ground motion effect also caused some degree of direct damage to the bridge. In order to grasp the characteristics of the seismic response of the bridges in this earthquake, Midas civil is used to model the Dachangshan Bridge, Feilong Bridge, Lancang River Bridge of Hangzhou-Ruili Expressway and Lancang River Bridge on Dali-Ruili Railway, and the ground motion information of the two stations closest to the epicenter of the earthquake, namely, the BSL station and the YPX station, were selected and inputted to carry out the analysis of the seismic response. The locations of the four bridges are shown in **Figure 7**, and it can be seen that all four bridges are located in the seismic intensity VI region. The latitude and longitude of each bridge, and the distance from the epicenter and stations are shown in **Table 2** (The epicenter is marked in black, bridges in blue, stations in red, intensity in blue lines and faults in red lines.).

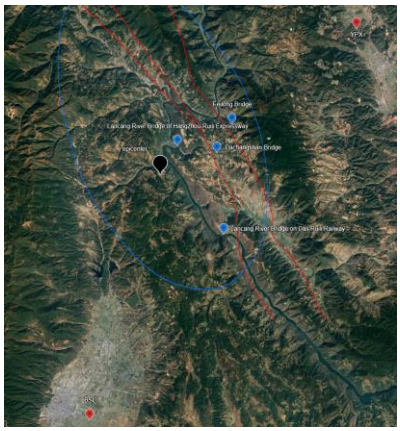

Figure 7. The location of YPX station, BSL station, bridges and epicenter.

Table 2. The coordinates of the bridges and their distance from the epicenter and stations.

Bridge	Dachangshan Bridge	Feilong Bridge	Lancang River Bridge of Hangzhou-Ruili Expressway	Lancang River Bridge on Dali-Ruili Railway
latitude and longitude	99.35° E 25.38° N	99.37° E 25.41° N	99.30° E 25.38° N	99.36° E 25.29° N
Distance from the epicenter (km)	7.7	10.8	4.5	10.1
Distance from YPX station (km)	20.4	17.0	23.6	27.1
Distance from BSL station (km)	34.3	37.9	33.2	26.7

3.1. Modelling of bridges and seismic response

3.1.1. Dachangshan Bridge

Dachangshan Bridge, a deck arch bridge, with a north-west direction of 11 degrees, and a main span of 141 m, 7.7 km from the epicenter, is located in the Hangzhou-Ruili Expressway section of Yongping County, Dali Bai Autonomous Prefecture, Yunnan Province. Referring to the paper of Huang et al. [16], the bridge is modeled by Midas civil, with a span of 141 m. The whole bridge is modeled by beam elements, with a total of 559 elements and 591 nodes. The bridge deck and arch ring are made of C40 concrete, and the columns are made of C25 concrete. The arch foot and the bottom of the abutment are fixed, and the deck slabs are rigidly connected with the cap beam. The deck slabs of this bridge are continuous. The natural vibration period is 1.273 s. The location of Dachangshan Bridge and the modeling of the main span are shown in **Figure 8**.

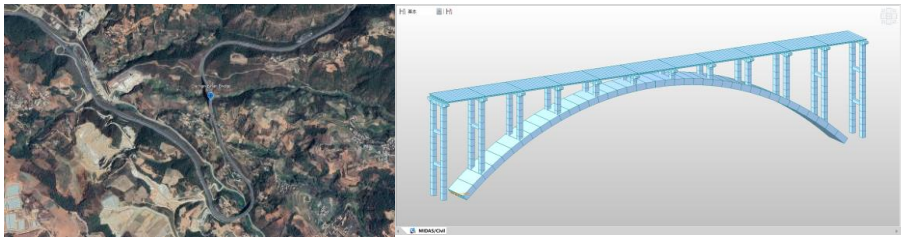

Figure 8. The location of Dachangshan Bridge and the modeling of the main span.

The analysis of seismic response is carried out by inputting the strong earthquake records measured by YPX station. The maximum bending moment is at the arch footing, 2.387×10^6 kN·m in the longitudinal direction and 1.338×10^7 kN·m in the transverse direction. The analysis of seismic response is carried out by inputting the strong earthquake records measured by BSL station. The maximum bending moment occurs at the arch footing, which is 1.391×10^6 kN·m in the longitudinal direction and 7.349×10^6 kN·m in the transverse direction.

The seismic responses of the bridge in the longitudinal and transverse directions corresponding to the seismic information of the two stations are shown in **Figure 9**.

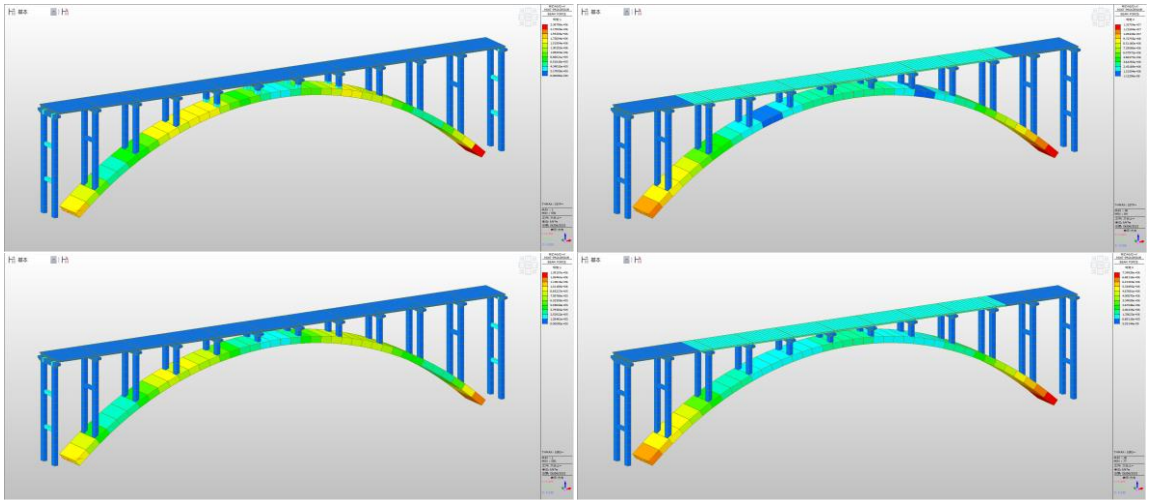

Figure 9. The seismic response in the longitudinal direction and the transverse direction corresponding to the seismic information of YPX station and BSL station.

3.1.2. Feilong Bridge

Feilong Bridge is a deck arch bridge, with a direction of 1 degree north-west along the bridge, with a main span length of 155 m, 10.8 km from the epicenter, located in Yongping County, Dali Bai Autonomous Prefecture, Yunnan Province. The bridge is modeled by Midas civil, with a total of 960 elements and 960 nodes, beam elements were used to model the bridge with a span of 155 m, C40 concrete for the arch, and C30 concrete for the columns, C25 concrete for the bridge deck slabs. The arch footings and the bottom of the abutments are fixed, and the deck slabs are rigidly connected with the cap beams. The natural vibration period is 2.043 s. The location of Feilong Bridge and the modeling of the main span are shown in **Figure 10**.

Figure 10. The location of Feilong Bridge and the modeling of the main span.

The analysis of seismic response is carried out by inputting the strong earthquake records measured by YPX station. The maximum bending moment is at the arch footing, 3.978×10^6 kN·m in the longitudinal direction and 1.243×10^7 kN·m in the transverse direction. The analysis of seismic response is carried out by inputting the strong earthquake records measured by BSL station. The maximum bending moment occurs at the arch footing, which is 2.572×10^6 kN·m in the longitudinal direction and 1.215×10^7 kN·m in the transverse direction.

The seismic responses of the bridge in the longitudinal and transverse directions corresponding to the seismic information of the two stations are shown in **Figure 11**.

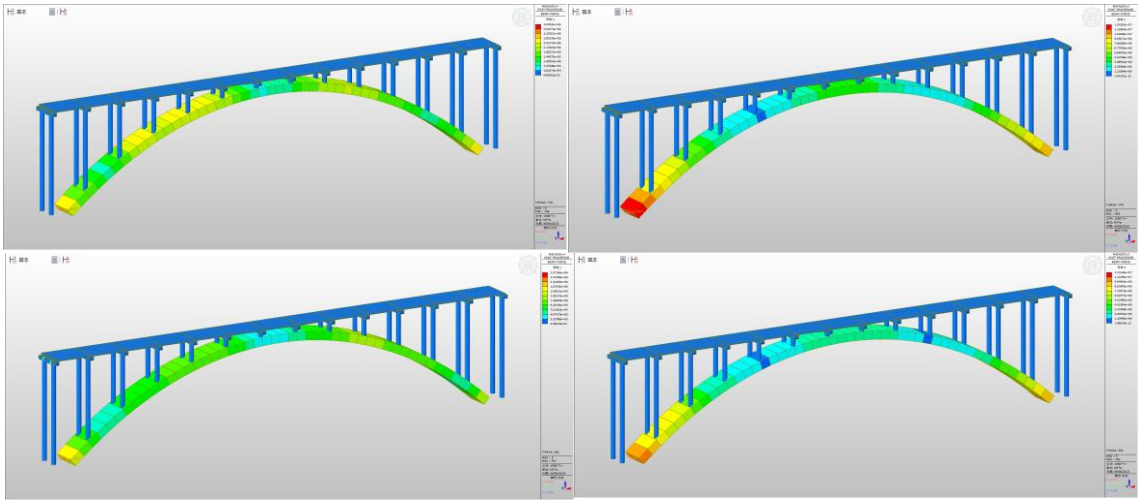

Figure 11. The seismic response in the longitudinal direction and the transverse direction corresponding to the seismic information of YPX station and BSL station.

3.1.3. Lancang River Bridge of Hangzhou-Ruili Expressway

Lancang River Bridge of Hangzhou-Ruili Expressway, a continuous rigid frame bridge, with the direction of 77 degrees north west along the bridge, with a total length of 426 m, a main span of 342 m and a height of 238 m. The bridge is 4.5 km from the epicenter of the earthquake, with steep mountains on both sides, and is a highway bridge for Hangzhou-Ruili Expressway across the Lancang River, which is located at the junction of Shanyang Township of Yongping County and Wayao Township of Longyang District, Baoshan City. It is the highest bridge on the Lancang River with the longest span bridge on the Dabao Highway. The bridge is a large-span asymmetric T-type continuous rigid frame bridge. The whole bridge is 436.6 m long, with a main span of 200 m, a deck width of 22.9 m and 83 m above the river. Referring to the paper of Xue [17], modeling was carried out using Midas civil, the total length of the bridge is 423 m, the main span is 200 m, the foundations are made of C30 concrete, the piers are made of C40 concrete and the bridge deck slabs are made of C50 concrete. The whole bridge was modeled by beam elements, with a total of 190 elements and 195 nodes. One end of the beam is fixed, the constraint of the other end is released in the longitudinal direction, and the foundation is fixed. Rigid connections are used between the foundations and the piers, and between the piers and the beams. The beams adopt variable cross-section group. The natural vibration period is 0.46 s. The location of Lancang River Bridge of Hangzhou-Ruili Expressway and the modeling of the main span are shown in **Figure 12**.

Figure 12. The location of Lancang River Bridge of Hangzhou-Ruili Expressway and the modeling of the main span.

The analysis of seismic response is carried out by inputting the strong earthquake records measured by YPX station. The maximum bending moment in the longitudinal direction is 3.478×10^7 kN·m at the connection between the main beam and the pier, and the maximum bending moment in the transverse direction is 5.084×10^7 kN·m at the foundation. The analysis of seismic response is carried out by inputting the strong earthquake records measured by BSL station. The maximum bending moment occurs at the foundation, which is 2.858×10^7 kN·m in the longitudinal direction and 7.108×10^7 kN·m in the transverse direction.

The seismic responses of the bridge in the longitudinal and transverse directions corresponding to the seismic information of the two stations are shown in **Figure 13**.

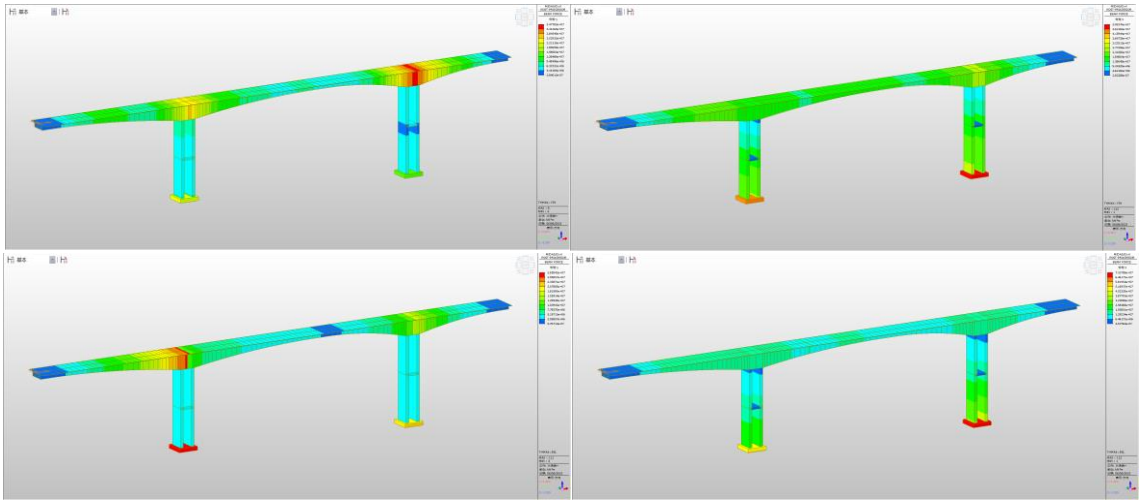

Figure 13. The seismic response in the longitudinal direction and the transverse direction corresponding to the seismic information of YPX station and BSL station.

3.1.4. Lancang River Bridge on Dali-Ruili Railway

Lancang River Bridge on the Dali-Ruili Railway is a railway bridge. It is a deck arch bridge with steel truss, which is 2 degrees north-east along the bridge direction. The bridge is 432 m long and 10.1 km from the epicenter. It is a bridge across the Lancang River on the Dali-Ruili section of the railway in Yunnan Province. It is situated between Yandong Township, Yongping County, Dali, Yunnan Province and Pingpo Township, Longyang District, Baoshan City, only about 100 m downstream from the Jihong Bridge. Referring to Xie [18], Midas civil is used for modeling. The whole bridge is modeled by beam element, with a total of 3071 units and 1580 nodes. The arch footings are fixed, the transverse and vertical displacements at both ends of the bridge deck are constrained. The span is 316.5 m, and the whole bridge is made of Q345 steel. The natural vibration period is 2.065 s. The location of Lancang River Bridge on Dali-Ruili Railway and the modeling of the main span are shown in **Figure 14**.

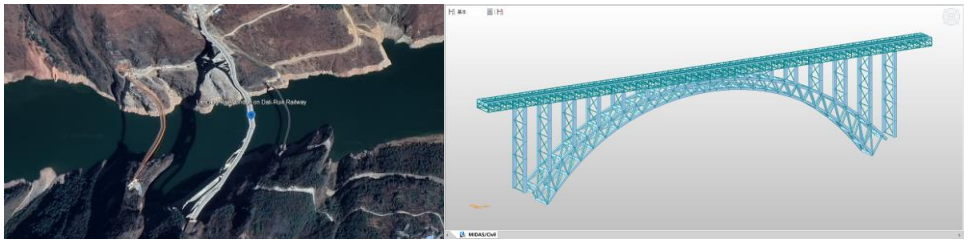

Figure 14. The location of Lancang River Bridge on Dali-Ruili Railway and the modeling of the main span.

The analysis of seismic response is carried out by inputting the strong motion records measured by YPX station. The maximum bending moment in the longitudinal direction is 7453.11 kN·m at the arch footing, and the maximum bending moment in the transverse direction is 2015.43 kN·m at the third span. The strong motion record measured by BSL station was inputted for seismic response analysis. The maximum bending moment in the longitudinal direction is 7453.11 kN·m at the arch footing, and the maximum bending moment in the transverse direction is 2015.43 kN·m at the third span.

The seismic responses of the bridge in the longitudinal and transverse directions corresponding to the seismic information of the two stations are shown in **Figure 15**.

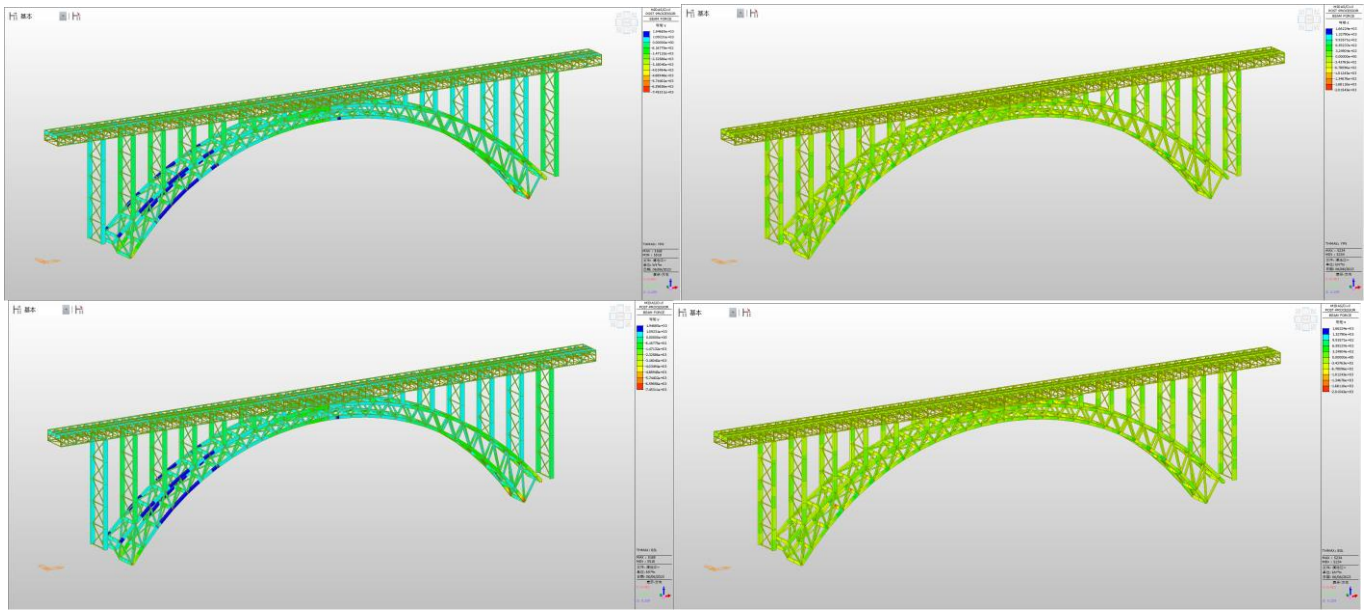

Figure 15. The seismic response in the longitudinal direction and the transverse direction corresponding to the seismic information of YPX station and BSL station.

3.2. Displacement of bridge structures and directivity of earthquake

Mode participation mass of Mode 1–10 of the four bridges are shown in **Table 3** (Direction x for longitudinal direction. Direction y for transverse direction. Direction z for vertical direction.).

As can be seen from **Table 3**, the bridges are mostly subjected to displacement and bending deformation in the longitudinal and transverse directions. The period of the first significant deformation of each bridge structure is shown in **Table 4**.

Table 3. Mode participation mass (%).

Bridge		**Dachangshan Bridge**			**Feilong Bridge**			**Lancang River Bridge of Hangzhou-Ruili Expressway**			**Lancang River Bridge on Dali-Ruili Railway**		
Direction		x	y	z	x	y	z	x	y	z	x	y	z
Mode	1	32.6	0	0	42.8	0	0	83.1	0	0	0	58.3	0
	2	0	77.1	0	0	0	0	0	56.8	0	2.17	0	0
	3	0	0	0	6.49	0	0	0.11	0	7.72	2.11	0	0
	4	0	0	0.49	0	78.4	0	0	0.1	0	17.3	0	0.09
	5	0	0.73	0	0	0	0	2.03	0	6.57	1.47	0	0
	6	28.0	0	0	0	0	0.02	0.76	0	6.87	25.0	0	0.38
	7	1.67	0	0	0	0.33	0	0	14.06	0	0	0.2	0
	8	0	0	0	0.48	0	0	0.85	0	3.12	0.64	0	0.46
	9	0.44	0	0	0	0	0	2.64	0	0.33	0	20.4	0
	10	0	0	2.2	1.28	0	0	0	0.8	0	0.42	0	0.15

Table 4. The period of the first significant deformation of each bridge structure (s).

bridge	**structure**	**direction**	**Period**
Dachangshan Bridge	Structure on the arch	longitudinal	0.579
		transverse	1.173
	arch	longitudinal	0.374
		transverse	1.173
Feilong Bridge	Structure on the arch	longitudinal	2.253
		transverse	1.842
	arch	longitudinal	0.5
		transverse	1.842
Lancang River Bridge of Hangzhou-Ruili Expressway	Structure on the arch	longitudinal	2.811
		transverse	1.781
	arch	longitudinal	2.811
		transverse	0.223
Lancang River Bridge on Dali-Ruili Railway	Structure on the arch	longitudinal	1.603
		transverse	2.065
	arch	longitudinal	0.398
		transverse	1.207

In order to study the correlation between the structural response of the bridge and the directionality of the earthquake, schematic diagrams of the correlation between the structural response of the bridges and the directionality of the earthquake were drawn, with the omnidirectional displacement response spectra as the base, and the directions of the bridge in the longitudinal direction and in the transverse direction are labelled (black straight lines are in the longitudinal direction, and the white straight lines are in the transverse direction), and the corresponding period of the bridge structure's first occurrence of the displacement response is labelled (labelled on the straight lines), and some of the results are shown in **Figures 16** and **17** [19,20].

The structural displacements of each bridge under the action of strong ground motion from YPX and BSL stations are shown in **Tables 5** and **6**.

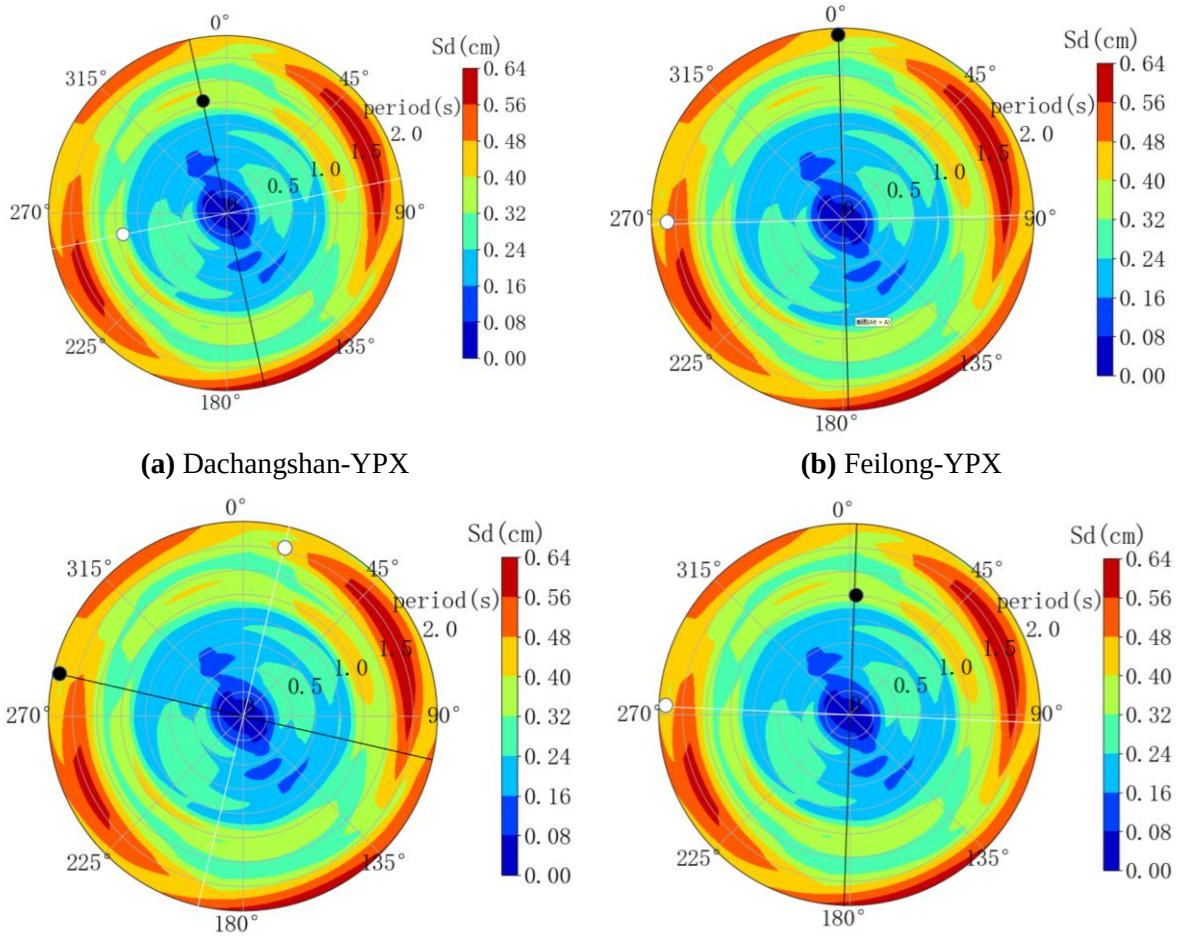

(a) Dachangshan-YPX **(b)** Feilong-YPX

(c) Hangzhou-Ruili-YPX **(d)** Dali-Ruili-YPX

Figure 16. The correlation between the structural response of the bridge and the directionality from YPX station.

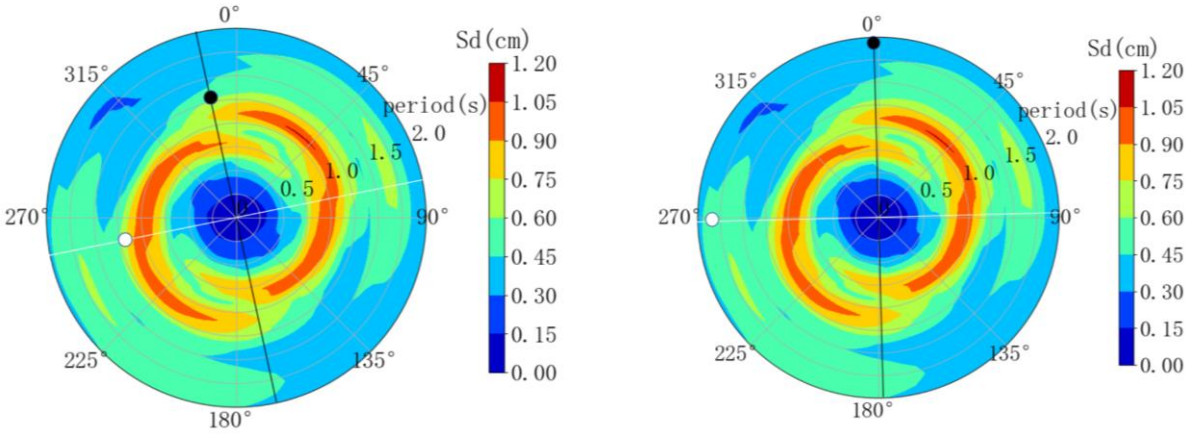

(a) Dachangshan-BSL **(b)** Feilong-BSL

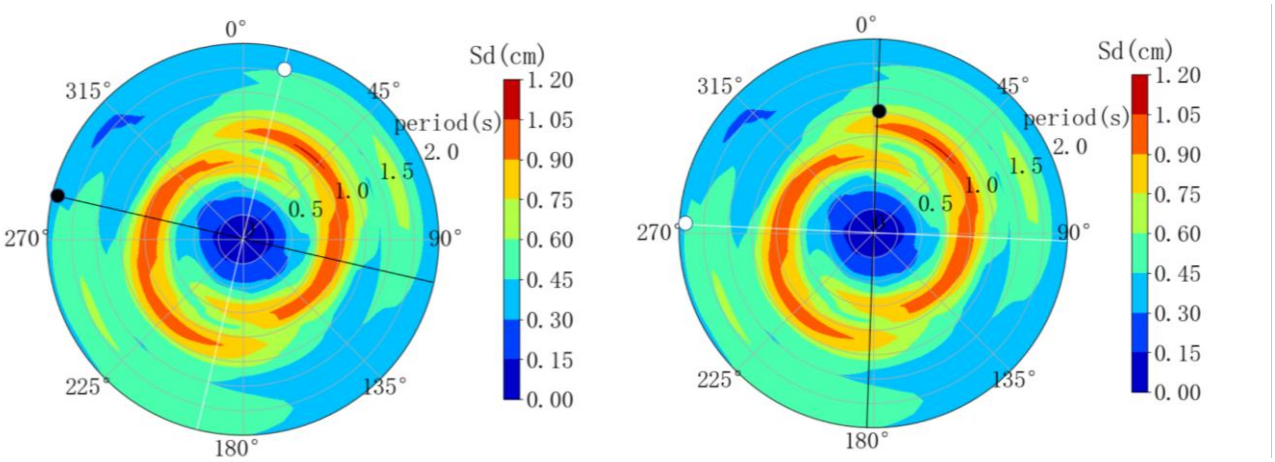

(c) Hangzhou-Ruili-BSL **(d)** Dali-Ruili-BSL

Figure 17. The correlation between the structural response of the bridge and the directionality from BSL station.

Table 5. The structural displacements of each bridge under the action of strong ground motion from YPX station (cm).

Bridge	Direction	1/4 of arch	1/2 of arch	3/4 of arch	North of beam	1/2 of beam	South of beam
Dachangshan Bridge	Longitudinal	2.619×10^{-3}	2.363×10^{-3}	2.569×10^{-3}	3.322×10^{-3}	3.945×10^{-3}	4.055×10^{-3}
	Traverse	3.172×10^{-3}	7.295×10^{-3}	3.172×10^{-3}	8.793×10^{-3}	9.424×10^{-3}	5.554×10^{-3}
Feilong Bridge	Longitudinal	1.028×10^{-3}	1.017×10^{-3}	8.880×10^{-4}	4.754×10^{-3}	2.166×10^{-3}	4.738×10^{-3}
	Traverse	1.557×10^{-3}	4.687×10^{-3}	1.557×10^{-3}	8.843×10^{-3}	5.653×10^{-3}	8.843×10^{-3}
Lancang River Bridge on Dali-Ruili Railway	Longitudinal	1.500×10^{-3}	1.400×10^{-3}	1.600×10^{-3}	1.500×10^{-3}	1.600×10^{-3}	1.600×10^{-3}
	Traverse	2.800×10^{-3}	6.000×10^{-3}	2.500×10^{-3}	9.000×10^{-4}	8.000×10^{-4}	1.100×10^{-3}

(a)

Bridge	Direction	Northern pier	Southern pier	North of beam	1/2 of beam	South of beam
Lancang River Bridge of Hangzhou-Ruili Expressway	Longitudinal	2.270×10^{-3}	2.442×10^{-3}	3.063×10^{-3}	3.141×10^{-3}	3.322×10^{-3}
	Traverse	7.130×10^{-4}	1.248×10^{-3}	3.697×10^{-3}	4.826×10^{-3}	6.365×10^{-3}

(b)

Table 6. The structural displacements of each bridge under the action of strong ground motion from BSL station (cm).

Bridge	Direction	1/4 of arch	1/2 of arch	3/4 of arch	North of beam	1/2 of beam	South of beam
Dachangshan Bridge	Longitudinal	1.340×10^{-3}	1.200×10^{-3}	1.294×10^{-3}	1.749×10^{-3}	1.720×10^{-3}	1.744×10^{-3}
	Traverse	1.696×10^{-3}	3.800×10^{-3}	1.696×10^{-3}	3.095×10^{-3}	4.854×10^{-3}	3.095×10^{-3}
Feilong Bridge	Longitudinal	4.960×10^{-4}	5.010×10^{-4}	4.660×10^{-4}	4.980×10^{-3}	1.627×10^{-3}	4.881×10^{-3}
	Traverse	1.461×10^{-3}	4.256×10^{-3}	1.461×10^{-3}	1.092×10^{-2}	5.042×10^{-3}	1.092×10^{-4}
Lancang River Bridge on Dali-Ruili Railway	Longitudinal	1.872×10^{-3}	1.861×10^{-3}	1.526×10^{-3}	1.642×10^{-3}	1.496×10^{-3}	1.754×10^{-3}
	Traverse	3.017×10^{-3}	6.184×10^{-3}	2.312×10^{-3}	1.057×10^{-3}	7.084×10^{-3}	1.033×10^{-3}

(a)

Bridge	Direction	Northern pier	Southern pier	North of beam	1/2 of beam	South of beam
Lancang River Bridge of Hangzhou-Ruili Expressway	Longitudinal	1.949×10^{-3}	2.989×10^{-3}	4.369×10^{-3}	4.385×10^{-3}	4.424×10^{-3}
	Traverse	8.460×10^{-4}	1.010×10^{-3}	1.990×10^{-4}	6.368×10^{-3}	1.020×10^{-4}

(b)

3.3. Comparison of seismic responses of four bridges

Dachangshan Bridge, Feilong Bridge and Lancang River Bridge on Dali-Ruili Railway are all deck arch bridges. With the influence of earthquake, the maximum bending moment of the three bridges in the transverse and longitudinal directions occur at the arch footing. Lancang River Bridge of Hangzhou-Ruili Expressway is a continuous rigid frame bridge. With the influence of earthquake, the maximum bending moment in the longitudinal direction of the bridge is at the connection between the main beam and the pier, while the maximum bending moments in the transverse direction are at the foundation.

Dachangshan Bridge and Feilong Bridge are deck concrete arch bridges, and the corresponding maximum bending moment in the longitudinal direction are smaller than those in the transverse direction when inputting the ground motion records from YPX station and BSL station for seismic response analysis. Lancang River Bridge on Dali-Ruili Railway is a deck steel truss arch bridge. The seismic response analysis is carried out by inputting the strong ground motion records measured by YPX station and BSL station. The maximum bending moment in the transverse and longitudinal directions of the bridge is smaller, and the maximum bending moment in the longitudinal direction of the two stations is larger than that in the transverse direction.

As a deck concrete arch bridge, the values of the maximum bending moment of the Feilong Bridge in the longitudinal and transverse directions corresponding to the strong ground motion record of the BSL station and the maximum bending moment values in the longitudinal direction corresponding to the strong ground motion record of the YPX station are larger than those of the Dachangshan Bridge. It can be seen that the larger the span of the deck arch bridge, the greater the maximum bending moment at the arch footing in the earthquake.

The corresponding period of the first transverse displacement response of Dachangshan Bridge is similar to the predominant cycle of the omnidirectional displacement response spectrum corresponding to the strong seismic record from BSL station, and the transverse direction of Dachangshan Bridge and the predominant direction of the omnidirectional displacement response spectrum corresponding to the strong seismic record from the two stations are very close to each other, which can be seen from **Table 6** that the displacement in transverse direction of Dachangshan Bridge is also obvious.

The first structural displacement response of Feilong Bridge and Lancang River Bridge on Dali-Ruili Railway has a period of about 2 s, and the predominant cycle of the omnidirectional displacement response spectrum corresponding to the strong seismic record from YPX station is 1.5 s. The direction of Failong Bridge and Lancang River Bridge on Dali-Ruili Railway is close to north-south, and they both have obvious displacement in transverse direction.

Feilong Bridge and Dachangshan Bridge are close to the north-south direction, close to the predominant direction of omnidirectional response spectrum at 0.25 s and 0.75 s from YPX station, and the motion should be stronger in the longitudinal direction; Lancang River Bridge of Hangzhou-Ruili Expressway is close to the east-west direction, approximately perpendicular to the predominant direction of omnidirectional response spectrum at 0.2 s and 0.4 s from BSL station, and Lancang

River Bridge on Dali-Ruili Railway is closely parallel to the fault, and motion should be strong in the transverse bridge direction.

4. Analysis of fragility

In recent years, small and medium sized earthquakes have occurred frequently in Baoshan, Yunnan. In order to study the future damage of the bridges under more severe earthquakes and the possibility of rapid repairing, the analysis of fragility of these four bridges are conducted. Analysis of fragility is a probability-based analysis method of structural seismic performance, which can show the relationship between structural seismic demand and seismic capacity [21]. According to the fragility curve, the damage probability of bridge with the action of earthquake can be calculated, then the seismic performance of the structure can be evaluated.

In this paper, based on the index of performance damage directly, the polynomial curve is used to fit the standard deviation, then the transcendental probability of different damage states of the structure is calculated to form the fragility curve of the structure. The IDA method needs to convert the selected seismic waves into multiple seismic waves with different amplitudes by adjusting the coefficients, and the converted seismic waves do not affect each other. The nonlinear time history analysis of the bridges is carried out by using the adjusted seismic waves, and the response of the bridges with the action of seismic waves of different intensities are obtained. The IDA curve can be obtained by regression analysis of the response of the bridges with the action of seismic waves of different intensities. The fragility curves of the bridges can be obtained by combining the relationship of the curve with the reliability theory. According to the fragility curve, the seismic performance of the bridges can be evaluated and predicted comprehensively. Related studies are as follows: Yan et al. [22] conducted fragility analysis for self-anchored suspension bridges. Long et al. [23] studied the relationship between the fragility of continuous girder bridges and the bearing, pier height and isolation. Zhang [24] studied the influence of different seismic isolation devices on the fragility curve of urban interchange ramp bridges.

The process of forming the fragility curve based on incremental dynamic analysis (IDA) is as follows:

(1) The bending moment-curvature curve of the cross-section is obtained by using XTRACT to analyze the cross-section, and the bending moment and curvature of the cross-section corresponding to the four damage states of no damage, slight damage, moderate damage and severe damage is obtained.
(2) The above six groups of ground motion records are taken, and each group of ground motion records contains three directions. Find out the direction of the maximum earthquake intensity, then adjust the maximum ground peak acceleration in this direction to 0.1 g, 0.2 g, 0.4 g, 0.8 g and 1.0 g, and adjust the acceleration in the other directions in equal proportions.
(3) The response of the bridge, i.e. the seismic response of the structure (the curvature of most dangerous section), is obtained by performing a nonlinear time course analysis of the established bridge model using a series of seismic waves obtained from the adjustments.

(4) The ratio of seismic demand to a certain damage index is calculated respectively, and it is plotted in the logarithmic coordinate system with the corresponding earthquake intensity index.

(5) The least square method is used to perform regression analysis on the above separate points, and the means and standard deviations are obtained, so as to obtain the exceedance probability according to the normal distribution.

The most dangerous cross-section of Dachangshan Bridge is the cross-section at the arch footing. The most dangerous cross-section of Feilong Bridge is the cross-section at the arch footing. The most dangerous section of Lancang River Bridge of Hangzhou-Ruili Expressway is cross-section at the bottom of the pier. The most dangerous section of Lancang River Bridge on Dali-Ruili Railway is the cross-section at the arch footing.

4.1. Calculation of capacity of the cross-sections

The curvature damage indexes for the most dangerous sections of the four bridges are shown in **Table 7**.

Table 7. The damage indexes of Bending moment-curvature for the most dangerous sections.

Bridges	**Direction**	**Index**	**The damage indexes**			
			No damage	**Slight damage**	**Moderate damage**	**Severe damage**
Dachangshan Bridge	Longitudinal	Bending moment (kN·m)	1.287×10^{4}	1.582×10^{4}	2.043×10^{4}	2.042×10^{4}
		Curvature (1/m)	1.032×10^{-3}	1.269×10^{-3}	2.566×10^{-3}	5.473×10^{-1}
	Transverse	Bending moment (kN·m)	4.544×10^{4}	7.598×10^{4}	8.360×10^{4}	8.349×10^{4}
		Curvature (1/m)	2.286×10^{-4}	3.824×10^{-4}	2.650×10^{-2}	2.746×10^{-2}
Feilong Bridge	Longitudinal	Bending moment (kN·m)	5.075×10^{4}	5.884×10^{4}	5.832×10^{4}	5.733×10^{4}
		Curvature (1/m)	1.343×10^{-3}	1.557×10^{-3}	3.072×10^{-2}	7.932×10^{-2}
	Transverse	Bending moment (kN·m)	1.776×10^{5}	2.186×10^{5}	2.143×10^{5}	2.062×10^{5}
		Curvature (1/m)	3.379×10^{-4}	4.158×10^{-4}	2.603×10^{-3}	8.387×10^{-3}
Lancang River Bridge of Hangzhou-Ruili Expressway	Longitudinal	Bending moment (kN·m)	2.236×10^{5}	2.555×10^{5}	2.463×10^{5}	2.268×10^{5}
		Curvature (1/m)	1.640×10^{-3}	1.874×10^{-3}	7.251×10^{-3}	2.975×10^{-2}
	Transverse	Bending moment (kN·m)	1.057×10^{6}	1.254×10^{6}	1.217×10^{6}	1.146×10^{6}
		Curvature (1/m)	2.780×10^{-4}	3.298×10^{-4}	1.502×10^{-3}	5.285×10^{-3}
Lancang River Bridge on Dali-Ruili Railway	Longitudinal	Bending moment (kN·m)	5.510×10^{4}	9.092×10^{4}	9.446×10^{4}	9.367×10^{4}
		Curvature (1/m)	1.220×10^{-3}	2.013×10^{-3}	1.340×10^{-2}	2.236×10^{-2}
	Transverse	Bending moment (kN·m)	4.130×10^{4}	6.822×10^{4}	7.083×10^{4}	7.021×10^{4}
		Curvature (1/m)	1.627×10^{-3}	2.687×10^{-3}	1.943×10^{-2}	3.022×10^{-2}

4.2. Fragility curves

The fragility curves of the four bridges are shown in **Figures 18** and **19**.

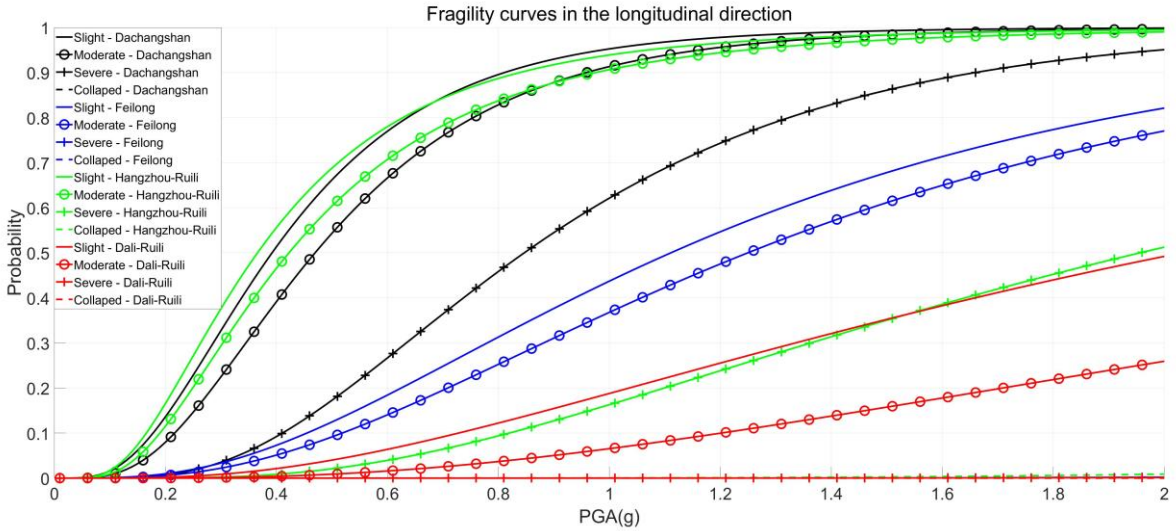

Figure 18. Fragility curves in the longitudinal direction.

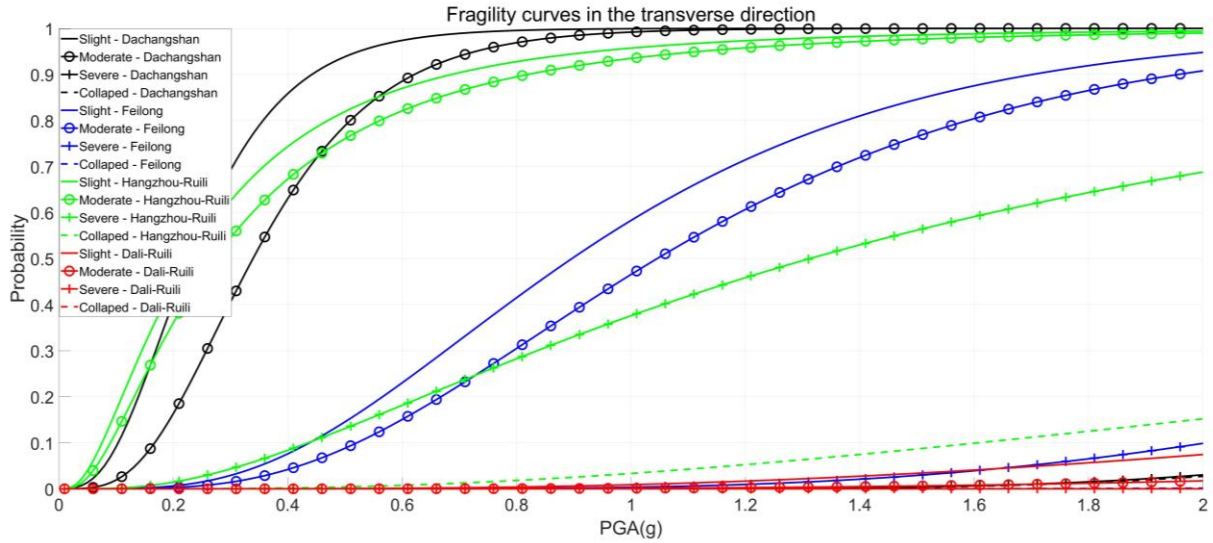

Figure 19. Fragility curves in the transverse direction.

Figures 18 and **19** are the fragility curves of the four bridges in the longitudinal and transverse directions, respectively. In the figures, different colors are used to represent the four bridges, and different lines are used to represent the damage levels. The abscissa represents PGA, and the ordinate represents the probability of different damage levels.

It can be seen from **Figure 18** that when PGA reaches 0.4 g, the probability of moderate damage in the longitudinal direction of Dachangshan Bridge and Lancang River Bridge of Hangzhou-Ruili Expressway reach more than 40%. When the PGA reaches 0.8 g, the Dachangshan Bridge has a high probability of severe damage. When PGA reaches 1.2 g, the probability of moderate damage of Feilong Bridge is only 50%. When the PGA reaches 1.4 g, the possibility of slight damage of the Lancang River Bridge on the Dali-Ruili Railway is about 30%.

It can be seen from **Figure 19** that when PGA reaches 0.4 g, the probability of moderate damage in the transverse direction of Dachangshan Bridge and Lancang

River Bridge of Hangzhou-Ruili Expressway reach more than 60%. When the PGA reaches 1 g, the probability of moderate damage of Feilong Bridge is 50%. When the PGA reaches 2 g, the probability of slight damage of the Lancang River Bridge on the Dali-Ruili Railway is below 10%.

From the comparison of **Figures 18** and **19**, it can be seen that with the same action of earthquake, that is, corresponding to the same PGA, the probability of the same level of damage in the transverse direction of Dachangshan Bridge is higher than that in the longitudinal direction, that is, Dachangshan Bridge is more prone to damage in the transverse direction than in the longitudinal direction.

Corresponding to the same PGA, the probability of the same damage level in the transverse direction of Feilong Bridge is higher than that in the longitudinal direction, that is, of the Feilong Bridge is more prone to damage in the transverse direction than in the longitudinal direction.

Corresponding to the same PGA, the probability of the same damage level in the transverse direction of Lancang River Bridge of Hangzhou-Ruili Expressway is higher than that in the longitudinal direction, that is, Lancang River Bridge of Hangzhou-Ruili Expressway is more prone to damage in the transverse direction than in the longitudinal direction, and there is a certain probability of collapse when PGA reaches 2 g.

Corresponding to the same PGA, the probability of the same damage level in the longitudinal direction of the Lancang River Bridge of the Dali-Ruili Railway is higher than that in the transverse direction, that is, the Lancang River Bridge of the Dali-Ruili Railway is more prone to damage in the longitudinal direction than in the transverse direction.

As shown in **Figures 18** and **19**, the Dachangshan Bridge is more likely to be damaged in the transverse direction than in the longitudinal direction under the same seismic effect. Under the same seismic effect, Failong Bridge is more likely to be damaged in the transverse direction than in the longitudinal direction. Under the same seismic effect, Lancang River Bridge of Hangzhou-Ruili Expressway is more likely to be damaged in the transverse direction than in the longitudinal direction, and has a certain chance of being collapsed when the PGA reaches 2 g. Under the same seismic effect, Lancang River Bridge on Dali-Ruili is more likely to be damaged in the longitudinal direction than in the transverse direction.

In general, the seismic performance of the bridge in the longitudinal direction is stronger than that in the transverse direction. Compared with the other three arch bridges, the seismic performance of Lancang River Bridge of Hangzhou-Ruili Expressway, the rigid frame bridge, is poorer. Although the three arch bridges are all deck arch bridges, the seismic performance of the steel truss bridge, Lancang River Bridge on Dali-Ruili is much stronger than that of the two concrete arch bridges, Dachangshan Bridge and Feilong Bridge. Although both are deck concrete arch bridges, the seismic performance of Feilong Bridge is better than that of Dachangshan Bridge.

5. Discussion and conclusion

The ground motion record from the BSL station of this earthquake shows that the predominant direction of the earthquake is northeast-southwest, which is perpendicular to the direction of the fault. The ground motion record from the YPX station show that the predominant direction of the earthquake is northwest-southeast direction, which is parallel to the direction of the fault. The predominant cycle is about 0.3 s.

The omnidirectional acceleration response spectra, omnidirectional velocity response spectra, and omnidirectional displacement response spectra of the BSL station show obvious directionality, and the predominant direction is approximately perpendicular to the direction of the fault. The omnidirectional representations of other indexes of intensity measure obtained from the strong motion records from the two stations also show obvious directionality, but it is mostly seen in the omnidirectional representation of displacement-related indexes of intensity measure cad (cumulative absolute displacement), and the predominant directions are perpendicular to the direction of the fault. The omnidirectional representation of displacements shows a clear directionality to the rupture of the ground motion.

Under the action of earthquake, the maximum bending moment of the continuous rigid frame bridge in the longitudinal direction is at the connection between the main beam and the pier, and the maximum bending moment in the transverse direction is at the foundation. During the construction of the bridge, the bending resistance of the foundation and the connection between the main beam and the pier should be strengthened. In the case of known earthquake-prone faults, for continuous rigid frame bridges perpendicular to the direction of the faults, attention should be paid to strengthening the bending resistance at the connection between the main beam and the pier. The direction of the continuous rigid frame bridge parallel to the direction of the fault should strengthen the bending resistance at the foundation.

Under the action of the earthquake, the arch footing of the deck arch bridge bears the maximum bending moment of the whole bridge, and under the same earthquake, the maximum bending moment of the deck arch bridge in the transverse direction is greater than that in the longitudinal direction. The larger the span of the deck arch bridge, the greater the maximum bending moment at the arch footing. The bending resistance at the arch footing should be strengthened during the construction of the deck arch bridge. The larger the span, the more the bending resistance at the arch footing should be strengthened. In the case of known earthquake-prone faults, the direction of the bridge should be perpendicular to the direction of the fault as much as possible to reduce the damage of the bridge under the action of ground motion.

The main span of Lancang River Bridge of Hangzhou-Ruili Expressway is 70 m shorter than that of Lancang River Bridge on Dali-Ruili Railway, but the maximum bending moment of the whole bridge is thousands of times that of Lancang River Bridge on Dali-Ruili Railway. It can be seen that the seismic capacity of continuous rigid frame bridge is much lower than that of deck steel truss arch bridge with the same span.

Compared with the deck concrete arch bridge, the bending moment of the deck steel truss arch bridge is smaller under the action of earthquake. This type of bridge has strong seismic capacity.

Comparison of the structural displacement of the bridges with omnidirectional response spectra of the strong motion record reveals that the bridges are more susceptible to damage when the corresponding period of the displacement response is similar to the predominant cycle of the strong motion record. In terms of bridge orientation, the Feilong Bridge and Dachangshan Bridge are orientated close to the direction of the fault, with strong vibration in the traverse direction.

The acceleration response spectra recorded by each station show that the PGA in all directions did not exceed the PGA of rare earthquake of six, so there is no clear seismic damage reported for these bridges in this earthquake. However, vulnerable location of the structure under the action of similar ground motion can still be known through this paper.

According to the vulnerability analysis in this paper, it can be found that the bridges are more vulnerable to be damaged in the transverse direction than in the crossover direction with the same seismic action; the rigid bridges are more vulnerable to be damaged than the arch bridges. The deck concrete arch bridge is more easily damaged than the deck steel truss arch bridge; although the maximum bending moment of Feilong Bridge is higher than that of Dachangshan Bridge, it is more difficult to be damaged than Dachangshan Bridge because of its own structure and reinforcement configuration. (the middle 4 spans are simply-supported beams).

In recent years, small and medium sized earthquakes have occurred frequently in Baoshan, Yunnan, and local bridges and other structures continue to face the risk of structural damage. Based on real bridges and real seismic data, the research and analysis in this paper compares the seismic response and vulnerability of different types of bridges, and provides some theoretical basis for the seismic design, construction and maintenance of these types of bridges. The site selection, design and construction of the bridge should consider the correlation between the direction of the bridge and the direction of the possible local seismic faults, with the action of earthquakes, the bridge is more prone to damage in the transverse direction. Limiting and vibration isolation devices should be appropriately installed at bridge abutments and other locations.

Although there is no obvious damage to the four bridges in this earthquake, the four bridges are close to the known faults. Therefore, the structural analysis and fragility analysis of the four bridges are carried out, and the structures that may be damaged in the new earthquake are speculated under the same geological conditions. Suggestions are made for the follow-up maintenance and reinforcement work. This is conducive to the resilience evaluation and rapid repair work after the damage caused by real earthquakes.

In the observation of the directionality of ground motion, more attention can be paid to displacement-related indexes of intensity measure.

Due to the limitation of space and the number of data, only the ground motion records of one earthquake are selected for research. If the ground motion records of multiple earthquakes in this area can be compared and analyzed, it may be possible to find the relationship between the omnidirectional representation of indexes related to

velocity and acceleration and the direction of the fault. In this paper, the response analysis of bridge structure based on numerical simulation is carried out. At present, communication with relevant departments is ongoing in order to use strain gauges and other measurement tools to study the real structural response of these four bridges under external forces to obtain a more realistic relationship between the structure and the direction of ground motion.

Author contributions: Conceptualization, YH and LT; methodology, YH; software, LT; validation, LT, YX and YW; formal analysis, YH; investigation, LT; resources, YX; data curation, YW; writing—original draft preparation, YH; writing—review and editing, LT; visualization, YX; supervision, YH; project administration, YH; funding acquisition, YH. All authors have read and agreed to the published version of the manuscript.

Funding: This research was funded by Open Foundation of National Engineering Research Center of High-speed Railway Construction Technology (Grant number: HSR202203), National Natural Science Foundation of China (Grant number: 52078498), Natural Science Foundation of Hunan Province of China (Grant number: 2022JJ30745), the Fundamental Research Funds for the Central Universities of Central South University (Grant number: 2020zzts149).

Acknowledgments: The authors acknowledge the Institute of Engineering Mechanics, China Earthquake Administration for providing the strong ground-motion data.

Conflict of interest: The authors declare no conflict of interest.

References

1. China Earthquake Networks Center (2023). Ms5.2 earthquake in Longyang District, Baoshan City, Yunnan Province. https://news.ceic.ac.cn/CC20230502232722.html.
2. Wang, D., Guo, X., Sun, Z., Meng, Q., Yu, D., et al. (2009). Damage to highway bridges during Wenchuan earthquake. Journal of Earthquake Engineering and Engineering Vibration,29 (03), 84-94.
3. Bao, M. (2010). Seismic response of simply-supported girder bridge subjected to near-fault pulse-like ground motion. (Master Thesis). Institute of Technology, Harbin.
4. Hu, J., Xie, L. (2011). Directivity in the basic parameters of the near-field acceleration ground motions during the Wenchuan earthquake. Chinese Journal of Geophysics,54(10), 2581-2589.
5. Li, S., Wang, J., Yan, X., Feng, Y. (2016) Influence of spatial distribution characteristics of near-fault ground motions on seismic responses of cable stayed bridges China Civil Engineering Journal,49(06), 94-104.
6. Zhang, F., Li, S., Yan, X., Wang, J. (2017) Effects of near-fault pulse-type ground motions on the seismic responses of a long span cable stayed bridge. Journal of Vibration and Shock, (36)21, 163-172+184.
7. Xie, J., LI, X., Wen, Z., Zhou, B. (2018) Variations of near-fault strong ground motion with directions during the 2013 Lushan Ms7.0 earthquake. Chinese Journal of Geophysics,61(04), 1266-1280
8. An, Z., Xie, J., Li, X., Wen, Z. (2019) Directivity effects on strong ground motion from the February 6,2018 Mw6.4 Hualien earthquake. Chinese Journal of Geophysics,62(12), 4658-4672.
9. Sun, M., Sun, B., Hou, G., Fan, F. (2020) Study on the main direction of ground motion and its effect on the dynamic response of structure. Chinese Journal of Geophysics,53(S2), 150-155.
10. Zhao, X., Wen, Z., Xie, J., Xie, Q., Liu, Y. (2021) Ground motion directionality in the 2018 Taiwan Hualien Mw 6.4 earthquake. Journal of Vibration and Shock,40(10), 235-243.

11. Li, G. (2023) Analysis of Vulnerability of Continuous girder bridges under Near Fault Ground Motion (Master Thesis). Institute of Engineering Mechanics, China Earthquake Administration, Harbin.
12. Inoue, K., Saitoh, K., Umeyama, Y., Igarashi, K., Ikeda, T. (2020) Evaluation of directionality considering periodic characteristics for strong motion observation records. Journal of Japan Society of Civil Engineers, Ser.A1(Structural Engineering & Earthquake Engineering (SE/EE)),76(4), I_205-I_213.
13. Huang, Y., Xie, Y., Tian, L., Wu, Y. (2023) Earthquake damage and enlightenment from traffic system in 2023 turkey Ms7.8 earthquake. World Earthquake Engineering, 39(03), 1-15.
14. Muho, V E., Kalapodis, A N., Beskos, E D. (2024) Multi-modal and multi-level structure-specific spectral intensity measures for seismic evaluation of reinforced concrete frames. Bulletin of Earthquake Engineering, 1-35.
15. Kulariya, M., Saha K S. (2024) Efficient intensity measures for vulnerability assessment of reinforced concrete buildings under flow-type and slow to moderately moving landslides. Structures,69107267-107267.
16. Huang, Y., Song, G., Li, G., Zu, L., Li, H., et al. (2022) Numerical Simulation of Performance of Arch Bridge during the 2021 Yangbi Earthquake. 2022 7th International Conference on Smart Grid and Electrical Automation,476-481.Lanzhou
17. Xue, H. (2021) Seismic vulnerability analysis of continuous rigid frame bridge based on IDA method (Master Thesis). Kunming University of Science and Technology, Kunming.
18. Xie, K. (2017). Seismic analysis and evaluation method of concrete filled steel tube arch bridge. Beijing: China Architecture & Building Press.
19. Magliulo, G., Maddaloni, G., Petrone, C. (2014) Influence of earthquake direction on the seismic response of irregular plan RC frame buildings. Earthquake Engineering and Engineering Vibration,13(2), 243-256.
20. Bradley, A B., Baker, W J. (2015) Ground motion directionality in the 2010-2011 Canterbury earthquakes. Earthquake Engineering & Structural Dynamics,44(3), 371-384.
21. Jeon, J., Choi, E., Noh, M. (2017) Fragility characteristics of skewed concrete bridges accounting for ground motion directionality. Structural Engineering and Mechanics,63(5), 647-657.
22. Yan, L., Cao, L., Yang, K. (2019) Seismic Fragility Analysis of Self-anchored Suspension Bridge Based on Incremental Dynamic Analysis. Journal of Chongqing Jiaotong University (Natural Science),38(11),41-45
23. Long, J., Ning, X., Shu, Y., Zhou, Y. (2023) Seismic vulnerability analysis of continuous girder bridge based on IDA method. Journal of Guizhou University (Natural Science),40(04), 108-117.
24. Zhang, H (2024) Seismic Vulnerability Analysis of Urban Interchange Ramp Bridges Based on IDA Approach (Master Thesis). Shijiazhuang Tiedao University, Shijiazhuang.